ANSI/AWS A5.1-91 E6013 Rutile Electrodes: The Effect of Wollastonite

Alterations to the coating composition were studied to determine the influence on diffusible hydrogen, operational behavior and all-weld-metal properties

BY N. M. R. DE RISSONE, I. DE S. BOTT, J. C. F. JORGE, P. CORVALÀN AND E. SURIAN

ABSTRACT. As there is not enough information about rutile electrodes in the international welding literature, this study has been carried out as part of a working program aiming to obtain fundamental knowledge about this system.

This study consists of the replacement of 0, 8 and 16% of quartz (100% SiO_2) with wollastonite (calcium silicate, 50% CaO/50% SiO_2) in the coating dry mix of three rutile ANSI/AWS A5.1-91 E6013 electrodes.

It was found that the increase of CaO in the covering produced the following:

- An increase in the slag basicity
- A decrease in silicon and oxygen all-weld-metal contents
- A diminution of the diffusible hydrogen in the weld metal
- A marked increment of all-weld-metal toughness.

In this way, the requirements of the Navy Industry International Register Grade 3 could be achieved and the minimal ANSI/AWS A5.1-91 E7018 toughness requirements were also satisfied.

The previously mentioned change in the coating composition also improved the performance of the electrode in the vertical welding position, though slightly deteriorated the flat welding position, with the typical excellent operational characteristics of rutile electrodes remaining constant.

Introduction

Despite a decrease in the use of manual covered electrodes that took place in some countries during the 1980s (Ref. 1), in Latin America, almost 80% of the deposited weld metal still originates from this type of welding consumable (Ref. 2). Accompanying the significant growth of steel production in China and India, a marked increase in manual electrode use has been observed (Ref. 3). Everything seems to indicate that the use of manual electrodes will stabilize to 30% of the deposited weld metal (Ref. 1).

Another interesting matter is that rutile coated electrodes, of the types ANSI/AWS A5.1-91 E6013 and E7024, continue to be required in a variety of markets. Some large manufacturers have replaced manual electrodes with solid and tubular continuous wires, but smaller ones still use manual electrodes due to the following reasons (Ref. 3):

- Simplicity, durability and low cost of the equipment required.
- Possibility of being used in open and closed spaces.
- It is relatively easy to find welders with the skill required for most applications.
- Wide range of consumables for most applications, which is a function of the quick fabrication setup.
- Availability in small units and at relatively low cost. It is generally accepted that welding consumables represent 1–2% of the final cost in general fabrication.

During the last 20 years, much work has been undertaken to acquire more knowledge about electrodes depositing C-Mn steels. Much attention was concentrated on the study of manual basic coated electrodes of the types ANSI/AWS A5.1-91 E7018 (Refs. 4, 5) and E7016 (Refs. 6, 7) leaving aside those of the rutile type. As far as the authors are aware, only a few papers about E7024 (Ref. 8) and E6013 (Refs. 9–13) type electrodes have been published in recent years with the aim of establishing the relationship among chemical composition, microstructure and mechanical properties of the deposited metal.

Taking into account that the welding consumable manufacturers manufacture larger amounts of rutile electrodes than basic ones, and in spite of the fact that the second type is technically more important than the first, it is necessary to develop a deeper and more complete knowledge about rutile electrodes due to the following reasons:

1) The unified requirements of the International Classification Societies (ABS, BV, DnN, LRS) (Ref. 14) establish three grades for the classification of rutile electrodes resulting from the temperature at which the 47 J minimum, on average, is obtained for the Charpy V impacts: Grade 1 at 20°C, Grade 2 at 0°C, and Grade 3 at –20°C. These demand a 33 J minimum for each individual value. Grade 3 is technically important because it is required by the naval industry. Not all manual electrode manufacturers have the "know-how" to satisfy, at least consistently, the requirements of the above-mentioned grade.

2) Nowadays, underwater wet welding is receiving a great emphasis. Basic electrodes are not adequate for this application. The most suitable electrodes for this purpose are the rutile type (Refs. 15, 16). It is therefore necessary to know the essential characteristics of these electrodes in order to be able to improve them.

3) On the other hand, all-position-welding flux cored wires are rutile types; consequently, their slags are also rutile (it is possible to get H_{DM} content under 5 mL/100 g of deposited metal). Using manual electrodes, the basic metallurgical

KEY WORDS

SMAW
E6013
Rutile Electrodes
Slag Basicity
Wollastonite
Calcium Carbonate
Coating Formulation
Microstructure
Mechanical Properties

N. M. R. DE RISSONE is with Universidad Tecnológica Nacional, Fac. Reg. de San Nicolás, Buenos Aires, Argentina; I. de S. BOTT is with Pontifícia Universidade Católica do Rio de Janeiro, Brazil; J. C. F. JORGE is with Centro Federal de Educação Tecnológica, CEFET/Rio, Rio de Janeiro, Brazil; P. CORVALÁN is with Research and Development, Conarco SA; and E. SURIAN is an Independent Consultant, Buenos Aires, Argentina.

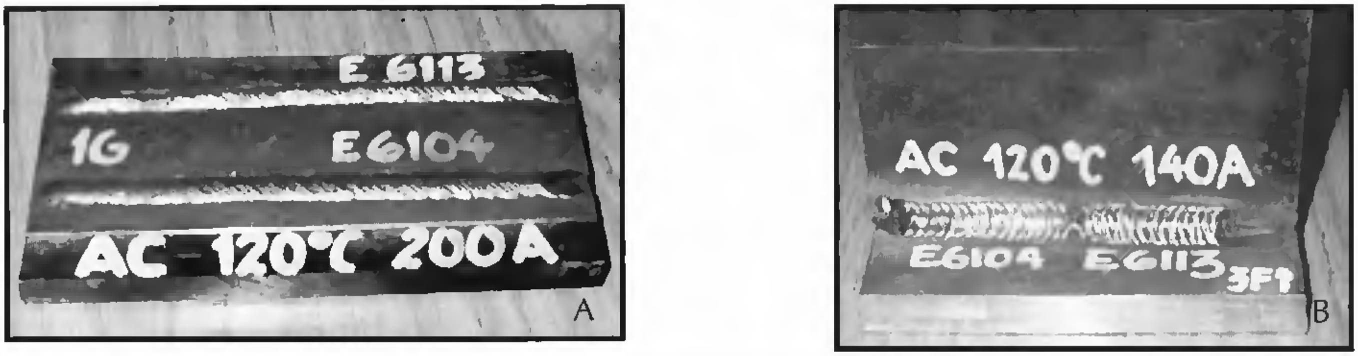

Fig. 1 — AC welding of E6104 (0-CaO) and 6113 (8-CaO) electrodes dried for 1 h at 120°C. A — Flat welding position; and B — uphill position.

knowledge could be obtained in a cheaper and simpler way than with the use of tubular wires, it being possible to transfer that knowledge to the latter second ones in the same way as has been done for the E7018 basic coated electrodes.

For these reasons we have initiated a research program with manual coated electrodes of the ANSI/AWS A5.1-91 E6013 type. Our previous step (Ref. 9) was to study the effect of varying the slag basicity of an E6013 electrode, on the all-weld-metal properties and operational behavior. This was done by increasing calcium carbonate from 5 to 15% at the expense of cellulose and Si-bearing materials of the covering dry mix. It was found that the increase in slag basicity produced an improvement in toughness without marked modifications to the microstructure. It was difficult to interpret the phenomena occurring due to the fact that there were simultaneously several opposing alterations in the coating. That is why, on this occasion, we have chosen a simpler and clearer approach to study how this fact may influence the electrode operational behavior, the mechanical properties and diffusible hydrogen of the weld metal: simply replacing quartz with wollastonite, which means SiO_2 with CaO, without any change in the rest of the coating component ingredients — rutile, cellulose, calcite and total metal constituent percentage.

Electrodes

Three electrodes, 4 mm in diameter and F = 1.50 (F = coating diameter/wire diameter), were designed replacing 0, 8 and 16% of quartz (100% SiO_2) with wollastonite (calcium silicate, 50% CaO/50% SiO_2) in the covering dry mix. This was done to obtain an increase in the basicity of the slag, through the replacement of SiO_2 with CaO. To maintain the operational characteristics of the rutile electrodes as much as possible, no change in the TiO_2 content was made.

Table 1 shows the electrode coating components and the slag chemical compositions of electrodes dried at 120°C for 1 h, with their corresponding Basicity Index, calculated according to Boniszewski (Ref. 17).

In all the tables and figures the electrodes are identified as follows: E6104 = 0-CaO, E6116 = 4-CaO and E6113 = 8-CaO. This takes into account the percentage of CaO incorporated in the electrode coating through wollastonite.

Table 1 — Coating Components and Slag Chemical Composition

	0–CaO	4–CaO	8–CaO
		Coating components	
Rutile	55	55	55
Calcite	7	7	7
Cellulose	6	6	6
Mn Powder	9	7.5	6
Fe Powder	7	8.5	10
Quartz	16	8	0
Wollastonite	0	8	16
		Slag chemical components[a]	
TiO_2	48.9	50.7	52.4
SiO_2	22.3	20.7	17.6
ZrO_2	0.28	0.32	0.29
Al_2O_3	0.35	0.21	0.20
MnO	11.6	9.2	8.0
K_2O	4.3	4.5	4.3
FeO	9.1	7.5	6.1
CaO	3.9	7.7	11.3
I.B.[b]	0.39	0.44	0.51

(a) These results correspond to the electrodes dried during 1 hour at 120°C, welded on AC, downhand position, from the fifth bead.

(b) IB = Boniszewski Basicity Index.

$$IB = \frac{CaO + MgO + BaO + SrO + Na_2O + K_2O + Li_2O + CaF_2 + 1/2\,(MnO + FeO)}{SiO_2 + 1/2\,(Al_2O_3 + TiO_2 + ZrO_2)}$$

Table 2 — Welding Parameters Used to Weld the ISO All-Weld-Metal Assemblies

Code	0–CaO		4–CaO		8–CaO	
Electrode	6104		6116		6113	
Current	AC	DCEN	AC	DCEN	AC	DCEN
Voltage (V)	26	23	24	22	27	23
Amperage (A)	198	182	200	185	200	196
Interpass temp. (°C)	70	70	70	70	70	70
Welding Speed (mm/seg)	4.3	3.5	4.0	3.4	4.2	3.5
Heat Input (kJ/mm)	1.2	1.2	1.2	1.2	1.3	1.3

Table 3 — The Parameters Used for Welding in the Flat Welding Position

		Amperage		Voltage	
Code	Electrode	AC	DCEN	AC	DCEN
0–CaO	6104	185	190	24	24
4–CaO	6116	200	195	22	25
8–CaO	6113	205	200	21	23

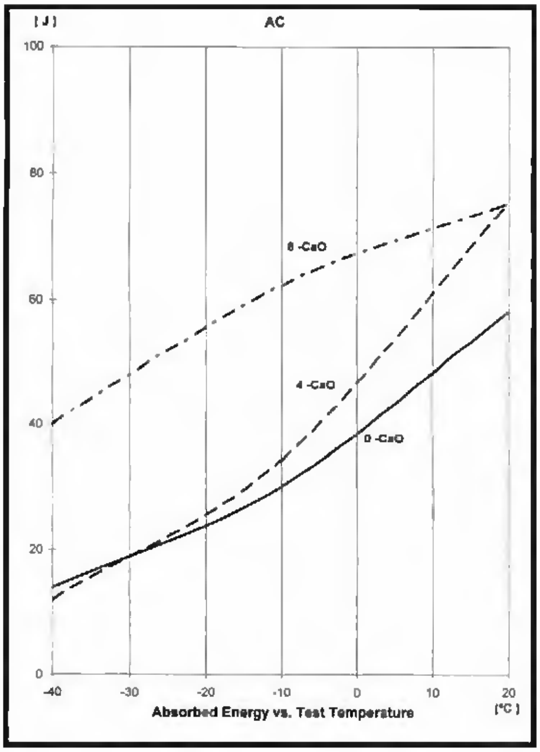

Fig. 2 — Absorbed energy vs. test temperature for AC welding.

Experimental Procedure

The working plan discussed below was carried out with the three electrodes mentioned previously.

Operational Behavior

The electrodes were tested for AC and DC electrode negative (DCEN) in the flat, uphill and downhill welding positions.

All-Weld-Metal Test Assemblies

Three passes per layer all-weld-metal test assemblies, according to the ISO 2560 standard (Ref. 18), were welded, in the flat welding position, using DCEN and AC. Table 2 shows the welding parameters used.

Chemical Composition

All the chemical analyses were performed on samples extracted from the all-weld-metal test assemblies.

Mechanical Testing

From each all-weld-metal test assembly, a Minitrac specimen (Ref. 19) and sufficient quantity of Charpy-V impact test pieces were extracted. The Minitrac specimen was tested at room temperature. The Charpy-V impacts were used to construct the Absorbed Energy vs. Test Temperature curve between −40° and 20°C.

Metallographic Study

To quantify the microstructural constituents of the columnar zones, in each weld, 30 fields of 100 points were measured at 500X by optical microscopy (Ref. 20). The percentages of columnar and refined zones were measured at 500X at the Charpy V-notch location. The columnar grain width was measured at 100X in the top bead as well as the thickness of the refined zones. The evaluation of recrystallized grain size was carried out according to the Linear Intercept Method (ASTM E112 standard). This entire study was performed on a cross section of the all-weld-metal test assemblies. Microhardness was determined on the same cut using the Vickers (1000 g) scale.

The inclusion analysis was carried out using a DSM960-Zeiss, SEM-dedicated Vidas image analyzer, with a calibration of 0.036 (μm/pixel, at 5000X magnification. For each weld, a total of 120 fields were examined, analyzing about 880 inclusions per sample. The analyzer automatically measured the maximum and minimum particle diameters, the shape factor and the areal analysis of the inclusion content. The data obtained with the analyzer was stored on disk and processed with a spreadsheet program. To undertake quantitative metallography of planar sections, it is necessary to take into account sectioning errors, which is the case in the present study. These results were corrected for sectioning errors according to the treatment proposed by Andrews (Ref. 21).

The weld metal inclusions were examined using energy dispersive spectrometry (EDS) microanalysis of single particles to determine their chemistry.

Diffusible Hydrogen

The measurements of diffusible hydrogen were performed according to the

Table 4—All-Weld-Metal Chemical Composition

Code	0–CaO		4–CaO		8–CaO	
Electrode	6104		6116		6113	
Current	AC	DCEN	AC	DCEN	AC	DCEN
C	0.063	0.058	0.061	0.059	0.070	0.057
Mn	0.51	0.50	0.48	0.45	0.47	0.42
Si	0.49	0.51	0.39	0.37	0.30	0.23
P	0.011	0.011	0.011	0.012	0.011	0.011
S	0.010	0.010	0.010	0.010	0.009	0.009
			ppm			
Cu	1042	1033	1006	987	1010	1040
Ni	523	532	531	520	533	450
Cr	183	200	202	200	180	170
Mo	120	122	121	121	110	110
V	180	182	179	178	200	180
Nb	80	80	80	80	80	70
Ti	157	157	166	163	190	180
Al	55	50	40	50	55	55
B	<10	<10	<10	<10	<10	<10
N	120	161	107	205	91	212
O	1024	858	871	750	713	670

Wire Chemical Composition

								ppm			
C	Mn	Si	P	S	Cu	Ni	Cr	Mo	Ti	N	O
0.053	0.29	0.070	0.010	<0.010	1190	946	217	214	73	72	136

IIW method (Ref. 22) with the three electrodes dried for 1 h at 120°, 220°, 320° and 420°C. The first temperature is the appropriate one for this electrode and the last one is generally used for basic coated electrodes.

Results and Discussion

Operational Properties

The operational behavior of the three electrodes was determined for DCEN and AC in the flat, uphill and downhill positions. As the properties that will be described varied with the changes in the slag basicity, only 0-CaO and 8-CaO electrodes will be mentioned, understanding that the 4-CaO condition is within the other two.

To obtain optimal operational behavior with each electrode, it was necessary to augment the amperage slightly as the basicity increased. The parameters used in the flat welding position are listed in Table 3.

Arc Characteristics

All the electrodes presented a stable arc for each type of current, but as the CaO increased, the arc became less aggressive, more crackly and softer. The 8-CaO electrode showed lower penetration. Under AC, the arc was softer than for DC. The differences in arc behavior between the 0-CaO and 8-CaO electrodes were more noticeable for DC than for AC welding.

Transfer Characteristics

Spray transfer was dominant in the three electrodes for both types of current. In the flat welding position, the transfer of 0-CaO was faster than for the 8-CaO one and the opposite happened in the uphill position: it took longer to deposit a bead with 0-CaO than with 8-CaO. All electrodes showed a faster transfer under DC than AC.

Spatter

As slag CaO increased, the spatter increased slightly in quantity and size. For DC this effect was more marked. In all cases spatter was cold (it was possible to remove it by brushing).

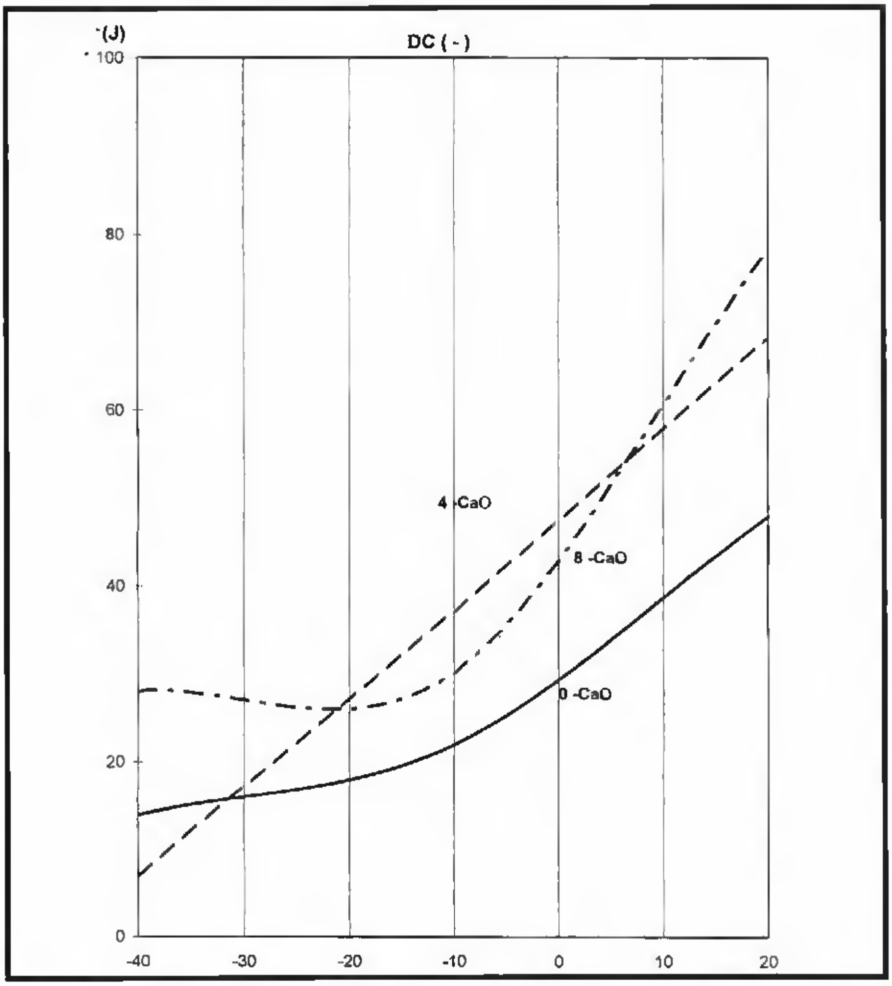

Fig. 3 — Absorbed energy vs. test temperature for DCEN welding.

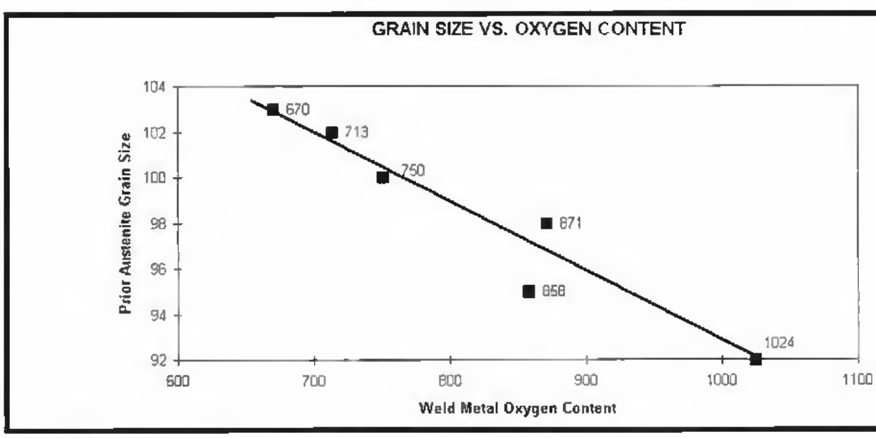

Fig. 4 — Grain size vs. oxygen content.

Table 5—Microhardness at Charpy V-Notch Location

		Columnar Zone		Refined zone			
				Coarse grain		Fine grain	
Code	Electrode	AC	DCEN	AC	DCEN	AC	DCEN
0–CaO	6104	180	186	170	187	166	179
4–CaO	6116	177	187	178	189	173	174
8–CaO	6113	176	190	174	193	166	182

Fig. 5 — Columnar zones in AC welding. A — E6104, 0-CaO; B — E6116, 4-CaO; and C — E6113, 8-CaO. (400X)

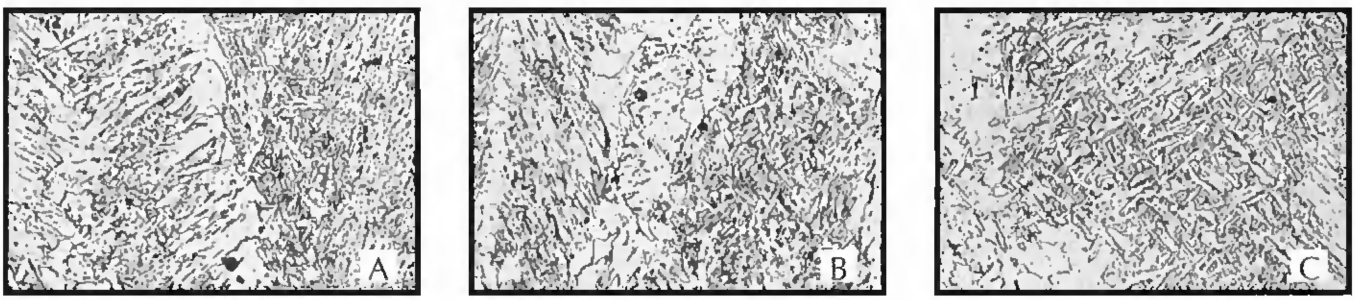

Fig. 6 — Columnar zones in DCEN welding. A — E6104, 0-CaO; B — E6116, 4-CaO; and C — E6113, 8-CaO. (400X)

Table 6—All-Weld-Metal Tensile Properties

Code	0–CaO		4–CaO		8–CaO	
Test	6104		6116		6113	
Current	AC	DCEN	AC	DCEN	AC	DCEN
Tensile Strength (N/mm^2)	534	594	528	563	533	563
Yield Strength (N/mm^2)	463	498	465	491	450	465
Elongation (%)	31.5	24.0	26.0	24.0	26.4	26.4

Slag Characteristics

As expected, all the slags were of the rutile type but with slight variations. They all completely covered the beads and the bead borders remained clean except with the 8-CaO electrode.

The 0-CaO slag was darker than the 8-CaO one, the latter having some small pores on its back face. This was not observed in the first case.

In the downhill position, the 0-CaO slag interfered with the welding pool less than did the 8-CaO slag. In the uphill position, the best slag behavior was presented by the 8-CaO. The 0-CaO slag was too fluid and tended to spill out.

The slag detachment was slightly better under AC than DC. For the former, the 0-CaO electrode showed self-detachment in the flat position; using 8-CaO the slag only cracked. In the horizontal fillet position the slag detachment was a little difficult in all cases.

Bead Characteristics

All the beads deposited on all types of current were well shaped with fine ripples. In the flat welding position, the more regular bead, with straighter borders, was achieved with the 0-CaO electrode, but in the uphill position, on the contrary, the flattest bead was obtained with 8-CaO for all current types. The 8-CaO electrode was a little better in the downhill position, but neither was really good.

Figure 1 shows typical beads.

It is very important to take into account that these electrodes have a good operational behavior but due to their overly simple formulas, they are not yet of operational complexity. To transform them into commercially competitive electrodes it would be necessary to sophisticate the formulas to improve the operational performance. In this case the objective was to investigate the effect that a simple replacement produced, in an attempt to isolate the behavioral tendencies.

Chemical Composition

Table 4 presents the all-weld-metal chemical composition obtained from mechanical property test specimens with electrodes under DCEN and AC.

It can be seen that, as a general tendency, the transfer of C, Mn and Si to the deposited metal was slightly higher for AC than DCEN (taking into account the results of each electrode on both types of currents), in spite of the fact that the oxygen values obtained for DCEN were lower than those achieved for AC, as expected, considering previous results (Ref. 8). N values were markedly lower for AC weldments than for DCEN ones, as was found with other types of electrodes (Ref. 23).

On the other hand, it was observed that as the slag CaO increased the deposited metal Si content decreased. This was probably due to two effects: the decrease of coating SiO_2 as it was replaced with CaO and the increase of slag calcium oxide (as wollastonite increased in the coating, Table 1); this decreased the activity of Si, which was transferred to the slag as oxide.

The oxygen values decreased with increasing CaO content for both AC and DCEN welding, that is to say with the expected slag basicity increase, taking into account previous results (Ref. 24). The nitrogen figures achieved for DCEN were similar to those presented in our previous work (Ref. 9) with E6013-type electrodes, and high if compared to the N values obtained with basic coated electrodes. It was thought (Ref. 25) that the higher N content of the rutile weld metal was due to the rutile assisting the transfer of nitrogen by the formation of TiN, which did not happen for AC.

The Mn contents are approximately of the same level (between 0.40 and 0.50%) for the three electrodes in spite of the increase in slag basicity, which would have produced a higher Mn transfer to the weld metal due to the oxygen content decrease, because the Mn content of the coverings was adjusted to obtain this result and to avoid introducing another variable to the system. This was because as the CaO increased it was necessary to incorporate less metallic manganese in the coating to obtain approximately the same figures in the weld metal (Table 1). As the slag CaO increased the metallic manganese content of the coating decreased from 9.0 to 6.0%.

The values of Cr, Ni, Mo, Cu, V, Nb, Al and B were not affected by the changes in the slag basicity. A slight increase of the Ti could be observed.

Mechanical Properties

Microhardness Properties.

Table 5 shows the microhardness values obtained for the different zones at the Charpy V-notch location. It was observed that with the slag CaO increase the microhardness figures of the other zones

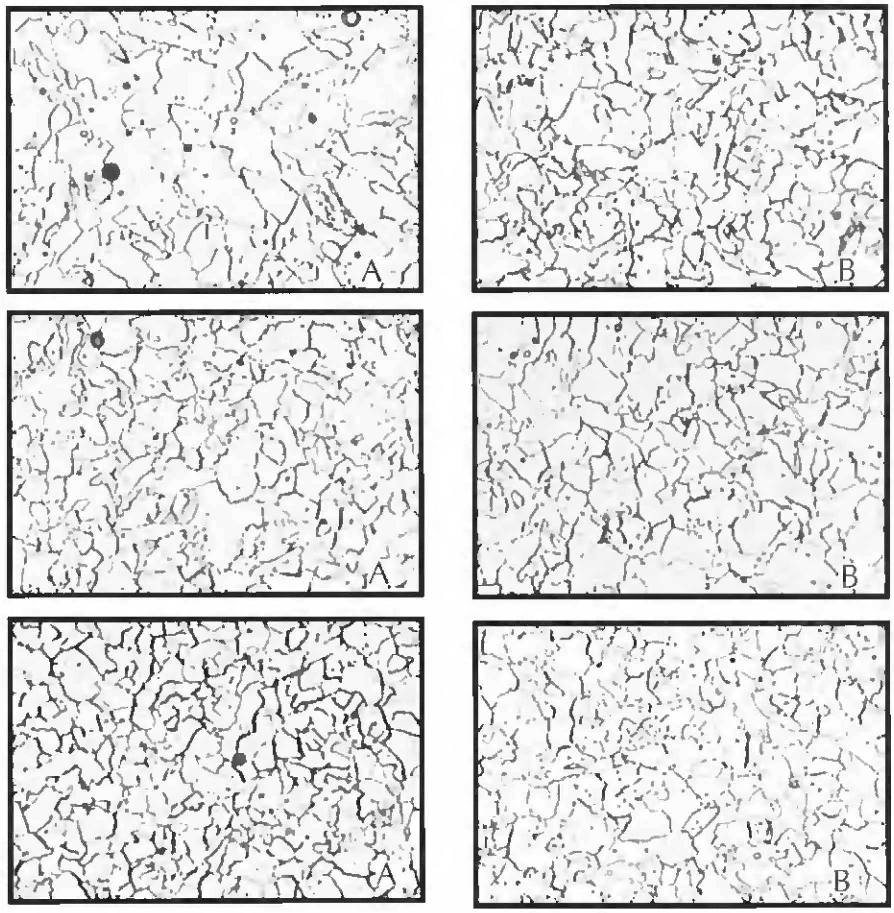

Fig. 7 — Fine grain refined zones for welding with AC (left-hand side) and DCEN (right-hand side) current. A — E6104/0-CaO; B — E6116/4-CaO; and E6113/8-CaO (640X).

Table 7 — Charpy-V Results

Ac Temp	0–CaO E6104	Avg	4–CaO E6116	Avg	8–CaO E6113	Avg
–40	12 10 12 15	12	10 12 9 10	10	15 75 30 55 21	39
–30	10 9 15 18	13	11 14 14 26	13	59 69 55	61
–20	20 24 20	21	22 40 10 25	24	65 67 90 35	64
–10	27 31 26 31 36 28 34	30	40 37 48 20 40 29 48 35	37	72 65 93 83 70 28	69
0	34 29 36 43 44 45	38	62 54 50 40 25 44 25	43	75 60 42 39	54
20	56 58 55 60 55 65	58	78 81 80 81 51 82	76	62 88	75
DCEN Temp	**0–CaO E6104**	**Avg**	**4–CaO E6116**	**Avg**	**8–CaO E6113**	**Avg**
–40	10 15	13	5 4 7 7	6	40 21 35 30 9	27
–30	9 15 10	11	33 30 20 17 10	22	21 18 35 24 60	32
–20	19 27 33 25 32 29 27	26	14 15 10	13	19 27 33 12	23
–10	22 35 31 24 32 12 27 20 12 17	23	26 55 35 30	37	22 35 31 24 32 51 51 36	36
0	25 32 29 27	28	63 33 60	52	25 33 36 26 25 54 20 38	32
20	59 45 43	49	75 72 78 50	69	78 84 81	81

Table 8—Percentages of Columnar and Refined Zones at the Charpy V-Notch Location

		Columnar Zone		Refined zone					
				Coarse grain		Fine grain		Total	
Code	Electrode	AC	DCEN	AC	DCEN	AC	DCEN	AC	DCEN
0–CaO	6104	23	26	22	20	55	54	77	74
4–CaO	6116	30	28	17	27	53	45	70	72
8–CaO	6113	29	23	12	18	59	59	71	77

Table 9—Percentage of Microstructural Constituents of the Top Bead Columnar Zones

		AF		PF (G)		PF (I)		FS (A)		FS (NA)		PF		FS	
Code	Electrode	AC	DCEN	AC	DCEN	AC	DCEN	AC	DCEN	AC	DCEN	AC	DCEN	AC	DCEN
0–CaO	6104	24	25	46	37	3	5	13	26	14	7	49	42	27	33
4–CaO	6116	28	26	39	37	6	6	19	22	8	9	45	43	27	31
8–CaO	6113	40	46	40	37	2	2	10	9	8	6	42	39	18	15

AF: Acicular ferrite
PF (G): Primary ferrite grain boundary
PF (I): Primary ferrite intragranular
FS (A): Ferrite with aligned second phase
FS (NA): Ferrite with nonaligned second phase
PF = PF (G) + PF (I) = Primary ferrite
FS = FS (A) + FS (NA) = Ferrite with second phase

(columnar and fine and coarse recrystallized regions) were not modified.

Tensile Properties

Table 6 presents the tensile property results of the six all-weld-metal deposits. All were within the expected ranges for this type of deposit, but in all cases the values obtained for AC were lower than those for DCEN, possibly reflecting the lower N values obtained for AC. The decrease of Si as the CaO increased was not really reflected in the tensile properties.

Toughness

The values obtained for Charpy-V are presented in Table 7 for AC and DCEN welding. The absorbed energy vs. temperature curves of the three electrodes are shown in Figs. 2 and 3 for AC and DCEN welding.

From these figures and the table an important improvement in toughness was observed as the slag CaO increased for AC. With the highest slag CaO this improvement was so marked that it was easy to satisfy the minimal average Register Society requirements of 47 J at –20°C, as well as the 33 J minimum for each individual value. The ANSI/AWS A5.1-91 E7018 toughness requirement of 27 J at –29°C was also accomplished with this electrode.

By contrast, the effect of improving toughness was not so marked for DCEN welding. It was possible to obtain a general increase in toughness with the addition of wollastonite but it was not enough to satisfy the mentioned requirements of the norms. At 0°C the best values of absorbed energy were achieved with the intermediate electrode (4-CaO); at –10°C, 4-CaO and 8-CaO electrodes showed the same Charpy-V values; and at –20, –30 and –40°C the highest values were obtained with the more basic one (8-CaO). At these last three temperatures toughness did not present an important variation: the change in the basicity of the slag seemed to produce a stable rise in toughness.

Metallographic Study

General

The percentage of columnar and refined zones at the Charpy V-notch location are shown in Table 8. The three electrodes for both currents were used with approximately the same heat input (Table 2). The percentages obtained for columnar and refined zones were almost the same in all the test specimens.

Columnar Zone

Table 9 shows the microstructural composition of the top bead columnar zones, in which the components have been quantified according to Ref. 20.

As the slag basicity increased, for AC welding, an increase of acicular ferrite at the expense of both primary ferrite and ferrite with second phase was found. For DCEN the same acicular ferrite increase was produced, mostly at the expense of ferrite with second phase, the primary ferrite remaining constant.

Analyzing the data of Table 9, it is observed that as the AF contents increased toughness increased, these results being in accordance with trends shown in previous works (Ref. 26).

Table 10—Average Width Values of the Prior Austenite Grains

		μm	
Code	Electrode	AC	DCEN
0–CaO	6104	92	95
4–CaO	6116	98	100
8–CaO	6113	102	103

The average widths of the columnar grains (the prior austenitic grains) in the same zones are shown in Table 10. The values obtained showed a slight increase as the CaO increased and the oxygen content decreased for both types of current, as shown in Fig. 4. With these rather high values of prior austenite grain size, a low quantity of primary ferrite and high percentages of acicular ferrite were observed as would be expected (Refs. 27–32). However, with the 8-CaO electrode, only 40–46 % of AF was obtained. This confirmed that the austenite grain size is not the only determining factor controlling this effect.

Figures 5 and 6 show typical micrographs of the columnar zones.

Reheated Zone

The refined top bead thickness figures are presented in Table 11. It is observed that as slag CaO increased there was no variation in the values obtained for AC and DCEN welding. Comparing both current results, it is noted that values were higher for DCEN, especially in the fine-grained zones.

The values obtained from the measurement of the refined grain size of the

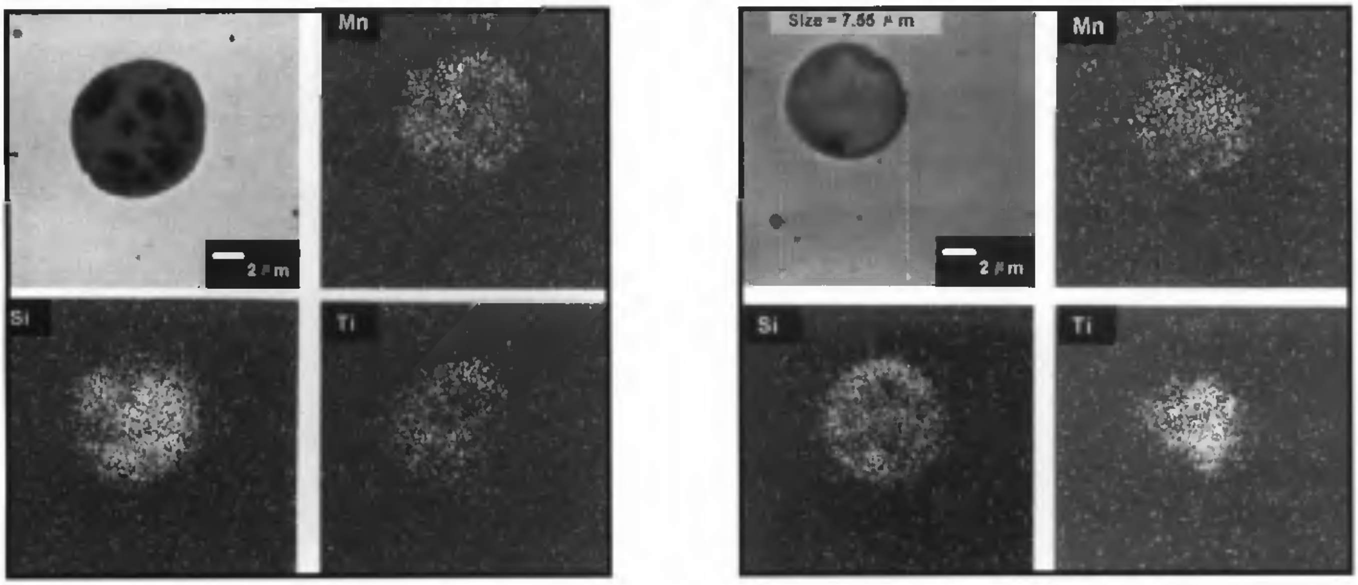

Fig. 8 — Typical X-ray mapping (Mn, Si and Ti) for spherical inclusions.

fine reheated zone are presented in Table 12. As the slag CaO increased, there was a decrease in the fine grain size for each current, these results being the same. This decrease could account for the improvement in toughness with the CaO increase as shown by the papers that described the effective contribution of the reheated region to the Charpy V-notch impact toughness in multirun welds (Refs. 33–36)

Figure 7 shows the micrographs of these regions.

It is generally accepted that toughness is related to several factors (Refs. 4, 5, 37, 38): hardness values, tensile properties, microstructural characteristics, and the type, quantity and size distribution of inclusions.

In this case, hardness and tensile values were very similar for the three electrodes and for both currents. The same happened with the percentages of columnar and recrystallized zones. But in the columnar zones, which constitute around 30% of the Charpy V-notch location, there was an increase of acicular ferrite at the expense of primary ferrite and/or ferrite with second phase, as the basicity of the slag increased, for AC and DC. The former microconstituent is recognized as one that improves toughness. On the other hand, the fine refined grain size of the recrystallized zone (which constitutes 55% of the Charpy V-notch location, with the total recrystallized region being about 70%) decreased with increasing CaO slag content. This fact can also account for improvement of toughness.

Table 11—Thickness of the Top Bead Refined Zones (mm)

		CG		FG		TRZ	
Code	Electrode	AC	DCEN	AC	DCEN	AC	DCEN
0–CaO	6104	0.50	0.55	1.15	1.25	1.65	1.80
4–CaO	6116	0.50	0.60	1.00	1.20	1.50	1.80
8–CaO	6113	0.55	0.60	1.10	1.30	1.65	1.90

CG: coarse grain
FG: fine grain
TRZ: total refined zone

Table 12—Values of Fine Recrystallized Grain Size (µm)

Code	0–CaO		4–CaO		8–CaO	
Electrode	6104		6116		6113	
Current	AC	DCEN	AC	DCEN	AC	DCEN
Diameter	8.7	8.1	8.0	7.4	6.9	6.7

Table 13—Chemical Composition of the Inclusions

WELD	6104 0–CaO		6116 4–CaO		6113 8–CaO	
Average composition (%)	AC	DCEN	AC	DCEN	AC	DCEN
Si	18.9	25.2	19.6	20.7	24.9	27.1
Ti	25.6	24.7	26.0	24.1	18.5	18.7
Mn	54.3	49.4	52.6	53.2	52.1	48.6
Al	0.8	0.8	1.1	0.9	2.0	1.6
S	0.4	0.0	0.3	0.4	0.4	0.8
Ca	—	—	0.3	0.5	0.2	1.2
K	—	—	0.2	0.1	1.8	1.9

Inclusion Analysis

The analysis of the role of inclusions on the final weld metal microstructure must take into account several phenomena related to different weld metal development aspects: from the sequence of deoxidization reactions in the welding arc, where the weld pool conditions are affected by many process variables, such as heat input and type of shielding (Refs. 39, 40), to the solid-state transformation characteristics.

Semiquantitative inclusion analysis is shown in Table 13. Mapping for Ti, Si and Mn did not reveal a specific sequence of precipitation, although the X-ray mapping (Fig. 8) showed similar distribution of the main elements Si, Ti and Mn, as previously reported (Ref. 39).

It should be noted that the weld 8-CaO, which yielded the highest acicular ferrite volume fraction, presented inclu-

Table 14—Inclusion Analysis, Oxygen Content, Acicular Ferrite and Prior Austenite Grain size

Weld		Austenite Grain Size (μm)	AF (%)	$d_{(mean)}$ 2D (μm)	$d_{(mean)}$ 3D (μm)	Total number of particles measured	Oxygen content (ppm)	Total Inclusion Vf
6104	AC	92	24	0.716	3.15	855	1024	1.59×10^{-2}
0–CaO	DCEN	95	25	0.655	1.66	940	858	1.11×10^{-2}
6116	AC	98	28	0.764	3.73	866	871	2.01×10^{-2}
4–CaO	DCEN	100	26	0.666	1.04	883	751	1.01×10^{-2}
6113	AC	102	40	0.715	1.15	952	713	1.16×10^{-2}
8–CaO	DCEN	103	46	0.566	0.95	802	670	0.61×10^{-2}

Table 15—Diffusible Hydrogen Values Obtained on AC

Drying Time	Diffusible H (mL H/100 g deposited metal) 0–CaO E6104	4–CaO E6116	8–CaO E6113
120°C	41.1	33.1	23.5
220°C	36.2	32.9	22.2
320°C	28.0	25.4	14.0
420°C	10.7	7.3	7.9

sions with the lowest Ti content, at least for the largest ones. A more detailed analysis is being carried out to clarify these tendencies.

SEM analysis revealed the presence of different phases of variable chemical composition within the inclusions. This pattern was present in most of the inclusions for a wide range of sizes, from 1 to 8 microns in diameter, and confirmed the heterogeneous nature of these inclusions. There was no surrounding envelope of different chemical composition from that of the central core, as reported previously (Refs. 39, 41).

It has been recognized that oxygen content affects the distribution (Ref. 29) and quantity (Refs. 42, 43) of inclusions and this can influence weld metal transformation. It is therefore expected that lower oxygen concentrations result in smaller inclusion diameter and lower volume fraction. This effect was found in the figures presented in Table 14, showing the results of inclusion analysis together with austenite grain size, oxygen content and percentage of acicular ferrite measurements. It can be seen that both the mean diameter and volume fraction of inclusions were the lowest for the 8-CaO weld metal, which had the lowest oxygen content.

In general, the highest slag basicity electrodes presented the lowest inclusion size and quantity.

Diffusible Hydrogen

Table 15 presents the results of diffusible hydrogen determinations. It can be observed that as the slag CaO content increased, the values of diffusible hydrogen decreased from 41 to 23 mL/100 g of deposited metal for the metal electrodes dried at 120°C. This was only obtained through the replacement of SiO_2 with CaO because the rest of the components of the dry mix formulations were not changed, unlike results presented in Refs. 9 and 10, where the increase of $CaCO_3$ was performed at the expense of cellulose, which is an important source of hydrogen. The quartz and wollastonite batches used in this work presented 0.22 and 0.32% loss at 1000°C, respectively. Thus, the initial hydrogen content of the electrodes was not varied with the replacement of SiO_2 with CaO or, at most, was only very slightly increased. It is important to remark that the simple replacement of SiO_2 with CaO, without any decrease of the coating H initial content, produced a diminution of the diffusible hydrogen.

When the electrode drying temperature was raised from 120 to 420°C it was possible to lower the diffusible hydrogen to less than 8 mL/100 g of deposited metal. This value corresponds to basic coated electrodes of the "low-hydrogen electrode" category (Ref. 44). Unfortunately, as these electrodes were dried at increasing temperatures some porosity began to appear as expected (Refs. 45, 46) due to the diminution of gas protection from the atmosphere, produced by the high-temperature drying process.

Conclusion

The coating composition of a standard ANSI/AWS A5.1-91 E6013-type electrode was modified through the replacement of quartz with wollastonite, that is to say SiO_2 with CaO. With the increase of the covering CaO content, and consequently that of the slag CaO, the following facts were observed:

- There was an improvement in the vertical position welding performance together with a slight detrimental effect on that of the flat welding position, but the typical excellent operational properties of rutile electrodes were maintained with all the electrodes for all the currents and welding positions.
- The all-weld-metal Si and O contents decreased for DCEN and AC, the former being lower than the latter. N values were similar in the three electrodes, but highest for DCEN.
- No important variation in the hardness values. Those obtained for AC were slightly higher than those for DCEN.
- No marked variation in tensile properties, these having been within the expected values for this type of electrodes.
- An important increase in toughness for both currents, especially noticeable for AC.
- No modification in the percentages of columnar and refined zones at the Charpy V-notch location.
- An increase in acicular ferrite content in the columnar zones on both AC and DCEN, as well as an increase in the prior austenite grain size.
- A decrease in the refined fine grain size for both AC and DCEN. This was similar for both currents.
- A decrease in the size and quantity of inclusions.
- A decrease in diffusible hydrogen for the weld metal deposited from the electrodes dried at 120°C.
- An important decrease in diffusible hydrogen as the drying temperature was increased.

Acknowledgments

The authors want to thank Conarco SA, Argentina, for the fabrication of the electrodes, Eng. Juan L. Trotti, Fundación Latinoamericana de Soldadura, for his cooperation and Miss María del Carmen Petruccelli for her help in the editing of this paper.

Author Ivani de S. Bott is grateful to CNPq (Conselho Nacional de Desenvolvimento Científico e Tecnológico) Brazil and to FINEP (Financiadora de Estudo e Projetos) Brazil, for financial support.

References

1. Myazaki, T. 1988. Flux Cored Wires for Robots. Hitachi Zosen Corp. Ariabe Works,

IIW Doc XII-1084-88.
2. Timerman, R., and de Vedia, L. 1991. Welding in Latinoamerica. Conferencia Internacional del Southafrican Welding Institute: Towards Cheaper Welding. Pretoria, South Africa.
3. Taylor, D. S. 1990. The role of MMA welding in 1990. *Welding and Metal Fabrication*, May, pp. 7–9.
4. Evans, G. 1990. Factors affecting the microstructure and properties of C-Mn all-weld-metal deposits. *Weld. Research Abroad*, WRC, 28.
5. Evans, G. 1990. The Effect of Alloying Elements on the Microstructure and Properties of Ferritic All-Weld-Metal Deposits. IIW Doc. II-A-817-90.
6. Taylor, D. S. 1982. The effect of manganese on the toughness of E7016 type weld metal. *Welding and Metal Fabrication*, 50(9): 452–460.
7. Surian, E., and Boniszewski, T. 1992. Effect of manganese and type of current on the properties and microstructure of all-weld-metal deposited with E7016-1 electrodes. *Welding Journal* 71(9): 348-s to 363-s.
8. Surian, E., Maraniello, E., and Boniszewski, T. 1995. The effect of carbon in E7024 SMAW electrode all weld metal. IIW-IIS Doc. II-A-905-94. *Welding Journal* 74(8): 279-s to 288-s.
9. Ramini de Rissone, N. M., Corvalan, P., and Surian, E. 1995. The effect of the Variation of the Slag Basicity on an AWS A5.1-91 E6013 Type Electrode. IIW Doc. II-A-929-94 (II-1262-95).
10. Boniszewski, T., Evans, G. M., and Hart, P. H. M. 1995. Studies of AWS E6013 Rutile Electrodes. Part 1: Effects of Calcium Carbonate. IIW Doc. II-A-931-94 (II-1263-95).
11. Boniszewski, T., and Evans, G. M. 1995. Studies of AWS Rutile Electrodes. Part 2: Changes in Toughness at Constant Strength. IIW Doc. II-A-940-95 (II-A-1263-95).
12. Boniszewski, T., and Evans, G. M. 1995. Studies of AWS Rutile Electrodes. Part 3: Deoxidation with Silicon. IIW Doc. II-A-948-95.
13. Boniszewski, T., and Colvin, P. 1995. Studies of AWS E6013 Rutile Electrodes. Part 4: Deoxidation with Magnesium. IIW Doc. II-A-949-95.
14. Rules and regulations for the classification of ships. *Lloyd's Register of Shipping*, January 1994 Edition.
15. Ibarra, S., Olson, D. L., and Grubbs, C. E. 1989. Underwater wet welding of higher strength offshore steels. OTC 5889, pp. 277–282, 21st OTC, Houston Tex., May 1–4.
16. Sanchez-Osio, A., Liu, S., Olson D. L., and Ibarra, S. 1993. Underwater wet welding consumables for offshore applications. 12th International Conference of Offshore Mechanics and Arctic Engineering. Book No. G0679A-1993.
17. Tuliani, S. S., Boniszewski, T., and Eaton, N. F. 1969. Notch toughness of commercial submerged-arc weld metal. *Welding Met. Fab.*, Aug., Vol. 37, pp 327–339.
18. ISO 2560-1973(E), *Covered Electrodes for Manual Arc Welding of Mild Steel and Low Alloy Steel — Code of Symbols for Identification*.
19. Schnadt, H. M., and Leinhard, E. W. 1963. Experimental Investigation of the Sharp-Notch Behaviour of 60 Steels at Different Temperature and Strain Rates. IIW-IIS Doc. 196-343-63.
20. Guide to the Light Microscope Examination of Ferrite Steel Weld Metals. 1988. IIW Doc. IX-1533-88.
21. Andrews, K. W. 1973. *Physical Metallurgy, Techniques and Applications*, Vol. II. Ed. George Allen. Unwin Ltd. p. 67.
22. IIW Commission II, Arc Welding. 1991. Measurement of Hydrogen in Ferritic Arc Weld Metal. IIW Doc. II-1155-91, The Hague 1991 Edition. Draft IIW/ISO Standard.
23. Losano, L. G., Raiter, V. E., and Boniszewski, T. 1989. Effect of the Use of Different Types of Wires on the Microstructure and Mechanical Properties of Basic Electrode Deposits. IIW Doc. II-A-792-89.
24. Eagar, T. W. 1978. Sources of weld metal oxygen contamination during submerged arc welding. *Welding Journal* 57 (3): 76-s to 80-s.
25. Blunt, F. J. 1995. Prediction of Weld Metal Area and Chemical Composition in C-Mn Steels: A Literature Survey. IIW Doc. II-A-956-95.
26. Svensson, L. E., and Gretoft, B. 1990. Microstructure and impact toughness of C-Mn weld metals. *Welding Journal* 69(12): 454-s to 461-s.
27. Ferrante, M., and Farrar, R. A. 1982. The role of oxygen-rich inclusions in determining the microstructure of weld metal deposits. *Journal of Material Sciences* 17: 3293–3298.
28. Harrison P. L., and Farrar, R. A. 1981. Influence of oxygen-rich inclusions on the austenite to ferrite phase transformation in HSLA steel weld metals. *Journal of Material Sciences*, Vol. 16, p. 2218s.
29. Liu, S., and Olson, D. L. 1986. The role of inclusions in controlling HSLA steel weld microstructure. *Welding Journal* 65(6): 139-s to 149-s.
30. Farrar, R. A., Zhang, Z., Bannister, S. R., and Barritte, G. S. 1993. The effect of prior austenite grain size on the transformation behaviour of C-Mn-Ni weld metal. *Journal of Material Science*. 28: 1385–1390.
31. Ricks, R. A., Howell, P. R., and Barritte, G. S. 1982. The nature of acicular ferrite in HSLA steel weld metals. *Journal of Material Science*, 17: 732–740.
32. Cochrane, R. C. 1982. Weld metal microstructures: A State of the Art Review. IIW Doc. IX-1248-82.
33. Jorge, J. C. F., Souza, L. F. G., and Rebello, J. M. A. 1993. A contribution to the study of the relationship toughness-microstructure of C-Mn weld metal. *Proceedings of the XIX Encontro Nacional de Tecnologia da Soldagem*, Brazil. pp. 1–19 (in Portuguese).
34. Jorge, J. C. F., Rebello, J. M. A., and Evans, G. M. 1993. Microstructure and Toughness Relationship in C-Mn-Cr All Weld Metal Deposits. IIW-Doc. II-A-880-93.
35. Zeeman, A., and Rebello, J. M. A. 1992. Microstructure and Toughness Relationship in C-Mn-Ni All Weld Metal Deposits. IIW-Doc. II-A-858-92.
36. Paranhos, R. P. R., and Rebello, J. M. A. 1984. Toughness-microstructure relationship of a C-Mn weld metal obtained from submerged arc multi-run welds. *Proceedings of the X ENTS*, pp. 95–115 (in Portuguese).
37. Abson, D. J., and Pargeter, R. J. 1987. Factors Influencing the As-Deposited Strength, Microstructure and Toughness of Manual Arc Welds Suitable for C-Mn Steel Fabrication. IIW Doc. II-1092-87.
38. Surian, E. S., and Boniszewski, T. 1992. Effect of oxygen content on Charpy V-notch toughness in 3% Ni steel SMA weld metal. *Welding Journal* 71(7): 263-s to 268-s.
39. Klunken, O., and Grong, O. 1989. Mechanisms of inclusion formation in Al-Ti-Si-Mn deoxidised steel weld metals. *Metall. Trans. A*. Vol. 20A, August, pp. 1335–1349.
40. Babu, S. S., David, S. A., Vitek, J. M., Mundra, K., and DebRoy, T. 1995. Development of macro and microstructures of carbon-manganese low alloy steel weld metals: inclusion formation. *Materials Sci. Technology*, Vol. 11, Feb., pp. 186–199.
41. Kayali, S., Colbert, J. M., and Kerr, H. W. 1982. Observation of inclusions and acicular ferrite nucleation in submerged arc HSLA welds. *Journal of Materials Science Letters*, Vol 2, pp. 126–128.
42. Ferrant, M., and Farrar, R. A. 1982. The role of oxygen rich inclusions in determining the microstructure of weld metal deposits. *Journal of Materials Science*, Vol 17, pp. 3293–3298.
43. Grong, O., and Matlock, D. K. 1986. Microstructural development in mild and low-alloy steel weld metals, *Int. Metals Review*, 31(1): 27–48.
44. International Standard ISO 3690-1977/Addendum 2. Published 1983/09/15.
45. Boniszewski, T. 1979. Manual metal arc welding — old process, new developments. Part II: understanding MMA electrodes. The Metallurgist and Materials Technology, 11(11): 640–643.
46. Pokhodnya, I. K., et al. 1975. Effects of the welding conditions, and the temperature at which rutile-coated electrodes are baked, on porosity in welds. *Avt. Svarka*, No. 8, pp. 34–37.